Journal of Magnetic Resonance **151,** 146–151 (2001)
doi:10.1006/jmre.2001.2329, available online at http://www.idealibrary.com on IDEAL®

COMMUNICATIONS

Spatial Dependence of a Differential Shading Artifact in Images from Coil Arrays with Reactive Cross-talk at 1.5 T

James Tropp* and Timo Schirmer†

*General Electric Medical Systems, 47697 Westinghouse Drive, Fremont, California 94539; and †General Electric Medical Systems, Goerresstrasse 35, Munich 80798, Germany

Received January 3, 2001; revised March 16, 2001; published online May 24, 2001

Reactive cross-talk causes leakage of the reception signal between neighboring coils of a receiver array. We present here experimental and computer-simulated NMR images (based upon a simple theory) to show, for an array of two coils, that the leakage (or secondary) signal is combined phase sensitively with the primary signal in each coil, to produce (in certain geometries) a differential shading artifact, manifest as a divot of missing intensity in the image derived from one (and only one) of the two coils. The asymmetry of this effect arises from the sense of the nuclear precession, and the afflicted coil may be swapped with its mate by reversing the direction of the static magnetic field. The artifact appears most clearly in transaxial images and is shown to be forbidden in certain types of saggital images. In a *simplified* theory for an array of two meshes (i.e., with only two degrees of freedom) the severity of the artifact depends upon the normalized coefficient of coupling (denoted η and related to the cross-talk in decibels, ψ, by $\psi = -20 \log \eta$.) While the presence of input trap circuits in a typical array doubles the degrees of freedom and complicates both the circuit theory and the circuit measurements, the cross-talk is nonetheless shown to be given by an expression of the form $\psi = -20 \log \eta'$, where the new primed parameter η' embodies the impedance-matching capacitance and the resistance of the scanner's preamplifiers, as well as the mutual reactance responsible for the cross-talk. The values of cross-talk inferred from the computer simulations of the image artifact are somewhat higher (by an estimated 3 to 6 dB) than those obtained by bench top measurements; but, given that the simulations unmistakably reproduce the unique and highly characteristic visual appearance of the artifact, the proposed model for its formation is claimed to be essentially correct. Finally, it is suggested that the artifact could be corrected by means of the filtered, edge-completed, reception profile described by Wald and co-workers (Wald *et al., Magn. Reson. Med.* 34, 433 (1995)).

Key Words: **image; artifact; array; coil; cross-talk.**

INTRODUCTION

Users of surface coils are familiar with the bands of shading, which appear in regions of the image where B_1 is parallel to B_0 (*1*). This shading occurs equally in isolated coils and in multicoil arrays and is independent of coupling between coils: furthermore, in some geometries (e.g., saggital images from spine arrays in horizontal-bore magnets) all coils may be equally affected (*2*).

We discuss here a different type of shading, which depends upon reactive coupling between coils, and so appears only in arrays. This effect is differential: that is, for a pair of coils, one loses, while the other gains intensity. (The coils reverse roles if B_0 is reversed.) Also, the form of shading is different from that of B_1/B_0 shading: the lost intensity appears as a divot rather than as a band. We will present a theory and calculations which account for the essential features of the differential shading and will also briefly discuss strategies for correcting the resulting intensity artifact.

Figure 1A is a schematic rendering of an array of two overlapped surface coils. When such an array is disposed about the axis of B_0, so that each coil is centered at a different value of the azimuth (as in Fig. 1B), differential shading will be observed in the axial images from individual coils, provided that they are mutually coupled by some stray reactance. If the array is rotated by $\pi/2$, about the vertical axis of the figure, and a saggital image is then recorded at center slice (through the meridian line of the coil pair), differential shading is *not* observed, regardless of the presence or absence of reactive coupling.

THE SIMPLIFIED THEORY OF THE ARTIFACT

To account for the differential shading, we adapt a theory of reactively coupled NMR coils, first given to explain the effect of cross-talk in laboratory-frame quadrature reception (*3*). Briefly, for a pair of identical resonant coils, coupled by parasitic mutual reactance, the strength of interaction is measured by the normalized coefficient of coupling η, defined as the product of the usual coefficient of coupling (in this case M/L, cf. Fig. 1C) and the source-loaded quality factor (i.e., at critical matching between the resonator and its driving source). Then for the circuit model in Fig. 1C, the cross talk ψ between coils, in decibels, is $-20 \log \eta$; and the response currents I_1 and I_2, for a pair of

1090-7807/01 $35.00

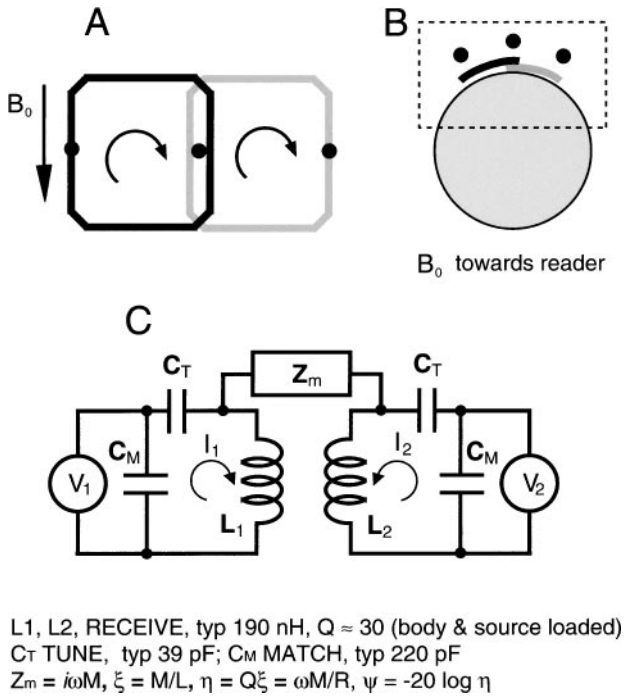

FIG. 1. Geometry (A and B) and circuit model (C) of the surface coil array. In A, the view from above: two flattened octagonal coils comprise the array, overlapped to minimize inductive coupling. The arrow points in the direction of the static *B* field; the black dots give positions of fiducial markers (vitamin capsules, cf. Experimental). B depicts the overlapped coils on the cylindrical phantom to be imaged. Black dots again are the fiducials; the dotted square shows roughly the region appearing in subsequent images. The view is of a transaxial slice cutting the coils and the phantom, with static field toward the reader. C shows a circuit model: two identical resonators, coupled by a mutual reactance, labelled Z_m, which is presumed inductive in this instance (capacitive would serve as well.) While the circuit topology as diagrammed could represent either surface or volume coils, the circuit parameters listed in figure are actually those of the surface the coil array used in this study. All losses are subsumed in the inductive *Q* factors, so that no resistive elements are shown explicitly. The drive voltages and response currents for Eq. [1] are also shown. Two mesh currents are indicated, corresponding to the two oscillatory degrees of freedom possessed by the circuit, although in principal there are four mesh currents.

complex drive voltages V_1 and V_2, are given (at center band) by the admittance matrix

$$\begin{bmatrix} I_1 \\ I_2 \end{bmatrix} = \alpha \begin{bmatrix} 1 & -i\eta \\ -i\eta & 1 \end{bmatrix} \begin{bmatrix} V_1 \\ V_2 \end{bmatrix}, \qquad [1]$$

where α is $1/\{R(1+\eta^2)\}$ and R is the net coil resistance ($\omega L/Q$), including any contributions coupled in by impedance matching to a source or load.

The voltages in Eq. [1] may represent either transmitter drive or emfs induced by precessing magnetization; also, there is no implied choice of coil type, so that surface or volume resonators may be specified. It will behoove us to maintain a flexible viewpoint. For example, with a homogeneous quadrature *volume* resonator in *transmission*, the two drive voltages will differ in phase by $\pi/2$ and are conveniently chosen to be $V_1 = 1$ and $V_2 = i$. Then by inspection of [1], the two quadrature channels must develop an asymmetry of response, with one producing a current of magnitude $(1+\eta)$ and the other of $(1-\eta)$. The coils are perfectly isolated, or decoupled, when $\eta = 0$; while at critical coupling, $\eta = 1$, the excitation of one member of the coil pair is perfectly nulled. Alternatively, if we consider the coils in reception, with the voltages arising from nuclear induction, then the signal from each coil is seen to be a sum of two components: (i) the primary, which would arise from the isolated coil, and (ii) a secondary component, coupled in from the neighbor coil, weighted by η, and phase-shifted by $\pi/2$.

Turning now to a pair of *surface* coils, reactive coupling between them also produces an asymmetry of response; and the mechanism described above still applies, but with the added complication that the signals received from individual voxels vary spatially in both magnitude and phase—assuming, of course, that the usual practice in array reception, of uniform excitation by an external volume coil, is followed (*1*). We may enunciate two necessary requirements for differential shading in a pair of surface coils: (i) reactive coupling between the coils and (ii) a spatial variation of signal phase from voxel to voxel in the imaging plane. (The second criterion explains why saggital images from the meridian plane of a spine array do *not* exhibit differential shading: the direction of B_1, and therefore the signal phase, is constant everywhere in the imaging plane.) In whatever geometry, a simple analytical calculation of the shaded images is not obviously possible for surface coils, so recourse is had to computer simulation, as we shall now describe.

In imaging with the two coils, we collect (for each phase encoding step) a pair of time records $I_1(t)$ and $I_2(t)$. The resulting data matrices (representing, for each coil, a two-dimensional *k* space) are then Fourier transformed; and since the two-dimensional FT is bilinear, Eq. [1] is seen to hold, voxel by voxel in real space, or point by point in *k* space. This bilinearity allows us to calculate theoretical images of the coupled coils by the simple expedient of applying the reciprocity theorem (*4*) to the B_1 profiles of the coils and the density function of the object to be imaged—utilizing the fact that the operation of Eq. [1] is that of combining, phase sensitively, the primary signal arising in each coil with the secondary (or leakage) signal coupled in from its mate, either in real space or in *k* space.

Specifically, for a sample of uniform magnetization, uniformly excited (i.e., by a homogeneous volume coil transmitter (*vide supra*)), the complex emf V_n induced in the *n*th coil, by a voxel located at position $\mathbf{r}$, is directly proportional to that coil's complex transverse B_1 field at $\mathbf{r}$,

$$V_n = \text{constant} \times \left[B_x^{(n)}(\mathbf{r}) + i\, B_y^{(n)}(\mathbf{r}) \right], \qquad [2]$$

where the subscripts *x* and *y* designate the transverse components of *B* and the superscript *n* identifies the coil in question. To apply reciprocity consistently to a coil pair, we require that the sense of the current be the same in both coils; this actually corresponds to excitation of the symmetric mode of the coupled pair. For the

voltages given in Eq. [2], the magnitudes of the response currents I_1 and I_2 are thus proportional to the image intensities from the individual coils, arising from the voxel at **r**. Since the required B_1 fields can be calculated quasi-statically, the theoretical image can be computed directly for different values of the coupling, η.

THE EFFECT OF INPUT TRAP CIRCUITS UPON CROSS-TALK

A typical array includes (for each reception coil) an input trap circuit, which serves the dual purposes of reducing cross-talk between array elements (*2*) and decoupling from the external transmitter field (*1*). In reception, the traps are passively activated by connection to a low impedance preamplifier ($\leq 5\,\Omega$) through a half-wave line, while in transmission a shunt diode (not shown in the subsequent figure) is activated to improve the blocking; in either case, the usual input nodes (the junctures of the preamps and half-wave lines) are effectively shorted, precluding a conventional measurement of cross-talk between array elements. An alternative measurement scheme, which mimics the operating conditions of the array, is shown in Fig. 2. With the preamps connected and activated, a low level (-50 dBm) RF carrier signal is coupled inductively into one of the receiver coils; the cross-talk in dB is then read directly by comparing the output signals of the two preamps, which are switched sequentially between a spectrum analyzer and a dummy load.

Some insight is gained by referring to the Kirchoff circuit equations, which are written in matrix form as: $\mathsf{K}\mathbf{I} = \mathbf{V}$, where **I** and **V** are, respectively, the column vectors comprising the mesh currents and applied voltages, and the Kirchoff matrix is given by

$$\mathsf{K} = \begin{bmatrix} i\omega L_1 + \frac{1}{i\omega C_M} + R_p & -\frac{1}{i\omega C_M} & 0 & 0 \\ -\frac{1}{i\omega C_M} & i\omega L_2 + \frac{1}{i\omega C_M} + \frac{1}{i\omega C_T} + R & i\omega M & 0 \\ 0 & i\omega M & i\omega L_3 + \frac{1}{i\omega C_M} + \frac{1}{i\omega C_T} + R & -\frac{1}{i\omega C_M} \\ 0 & 0 & -\frac{1}{i\omega C_M} & i\omega L_4 + \frac{1}{i\omega C_M} + R_p \end{bmatrix}, \qquad [3]$$

where R (taken as $\omega L/Q$ cf. Fig. 2) is the common series resistance of either receive coil, arising (chiefly) from body loading, R_p is the input resistance of the preamp, and the several other symbols are defined in the figure. For the setup as illustrated, the elements of the vector **V** are all zero save for the second, representing the applied carrier, whose amplitude we take as unity. Then, noting that the imaginary (i.e., reactive) elements on the diagonal of K must all vanish at the Larmor frequency, the following points may be verified: (i) Since no drive is ever applied in reception at meshes 1 or 4, the current ratios (I_2/I_1) and (I_3/I_4) are invariant. Therefore, the ratios (I_3/I_2) and (I_4/I_1) must be equal, so that ψ is $-20\log|I_4/I_1| = -20\log|I_3/I_2|$ where the straight brackets indicate the modulus of the complex quantity within. In terms of the circuit elements, the relevant current ratio is

$$I_3/I_2 = i\omega M/[R + 1/(\omega^2 C^2{}_M R_p)], \qquad [4]$$

which is equivalent to an expression given by Roemer *et al.* (*2*) to express the effect of the traps upon the isolation between coils. Note that in the absence of trapping, the expression in [3] devolves to $i\omega M/R$, which is just equal to $i\eta$ (cf. Eq. [1]).

It proves expedient to employ the primed symbol, η', for the quantity $\omega M/[R + 1/(\omega^2 C^2{}_M R_p)]$; and no objection will be found to writing the cross-talk for the four-mesh model as $\psi = -20\log\eta'$, by analogy with the simpler model of two meshes. Upon reflection, it will be seen that the two-mesh model predicts the correct current ratios and cross-talk for the four-mesh circuit, provided that we substitute η' for η in the computation.

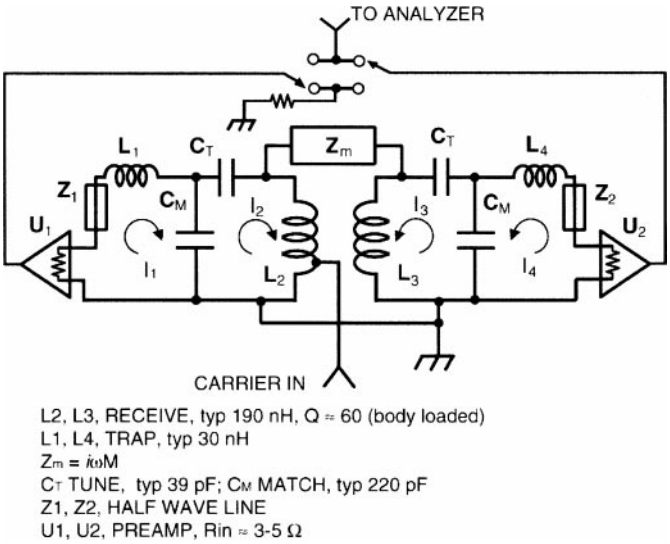

FIG. 2. Scheme for the measurement of cross-talk in an array terminated with low impedance preamplifiers. A carrier signal is coupled inductively (not necessarily by autotransformer, cf. Experimental) into one coil of the array; the outputs of each preamplifier are then measured sequentially; the difference in their output levels in decibels is the reported value of cross-talk. The symmetry of the experiment is checked by repeating the measurement sequence with excitation of the other array coil. Four mesh currents are shown, corresponding to the four oscillatory degrees of freedom for this circuit. The significant lossy elements are the resistance embodied in the Q factors of the receive coils and the input resistance of the preamps (shown but not labeled to avoid clutter). Trap diodes (cf. text) are also omitted.

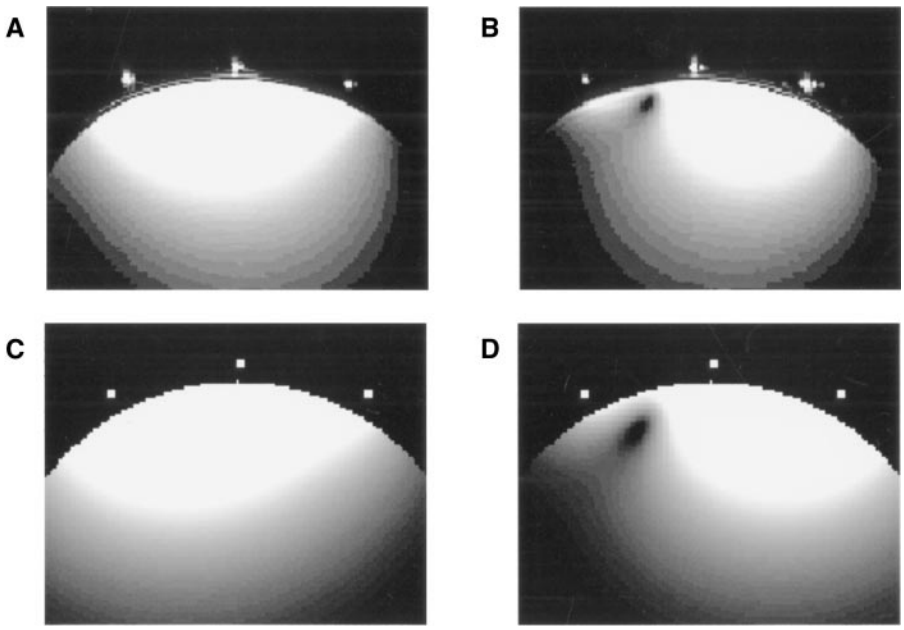

FIG. 3. Experimental and simulated images: in A and B, transaxial, gradient echo, proton images at 64 MHz, of cylindrical phantom (30 cm diameter), from individual coils ("left" in A and "right" in B) of the homebuilt array described in the text (cf. Experimental). The imaging parameters were TR = 400 ms, TE = 7 ms, field of view = 48 cm, image matrix 256 × 256 points. The phantom contains aqueous copper sulfate solution; the scanner was a GE Signa Horizon. (C and D) Computer-simulated images to match the experiment, with details as given in the text.

RESULTS

Figures 3A and 3B are experimental transaxial images of a cylindrical phantom, from the "left" and "right" coils of the array; the bright dots of intensity are fiducial markers and indicate (from left to right, for each image) the identical locations on the array (cf. Fig. 1). The images are windowed to emphasize the regions of overlapping intensity. The signal from the left coil (Fig. 3A) substantially invades the space bounded by its rightward mate, while the right coil does not respond symmetrically, but exhibits instead a divot of lost intensity, as shown in Fig. 3B. Essentially, signal intensity is transferred differentially from the right coil to the left. This effect is also observed in the computer simulations (Figs. 3C and 3D), whose geometry closely mimics that of the experimental set up. Intensity from the left coil extends strongly toward the right (Fig. 3C); while the missing divot is clearly seen in the right coil (Fig. 3D) Although the B_1 fields were calculated quasi-statically, and for filamentary currents, the overall impression is of close agreement (albeit not exact) between prediction and observation—particularly as regards the size and location of the divot.

However, the value of η' in the simulations of Fig. 3 was 0.2, while the bench top measurement (cf. Experimental and Fig. 2) gave a value of $\eta' \approx 0.1$ (i.e., from a cross-talk of -20 ± 2 dB), with the coils loaded as in the imaging experiment. The apparent discrepancy then, between the measured value of the cross-talk and that inferred from the simulations, is therefore 6 dB. For comparison, the predicted dependence of the artifact upon coupling strength is shown in Fig. 4, which gives

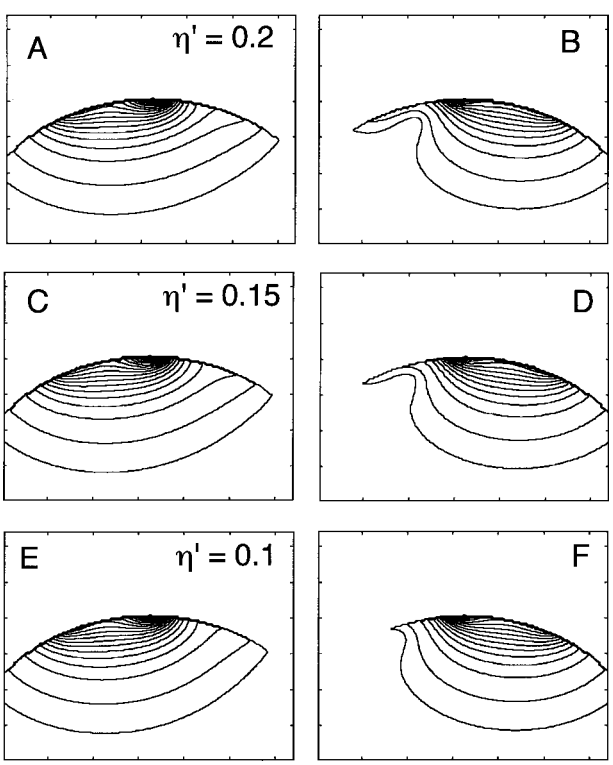

FIG. 4. Contour maps of simulated transaxial images at different values of the normalized coupling coefficient, η', grouped in pairs to correspond with earlier figures, i.e., Figs. 4A and 4B represent the left and right coils at an η' value of 0.2; and the rest of the layout, Figs. 4C and 4D at $\eta' = 0.15$, etc., follows the same self-explanatory scheme. Refer to the text for additional details.

contour plots of the simulated image intensities for the three values of η'—0.20, 0.15, and 0.10—corresponding to values of cross-talk between coils of −14, −16.5, and −20 dB. While the artifact is detectable at rather weak coupling (where it is more readily visualized in the contour map than in an image display), the characteristic bright finger of intensity, which demarcates the divot, is not yet visualized at $\eta' = 0.1$. It is seen clearly, however, at $\eta' = 0.15$, i.e., at a value of cross-talk about 3.5 dB above the nominal experimental value. Given that the accuracy claimed for the bench-measured cross-talk is ±2 dB, and that a range of cross-talk values, probably spanning 3 dB, could reasonably simulate the images, the overall discrepancy—between measurement and inference—could lie within a considerable range: from 1 to 8 dB, depending upon the stack up of errors and uncertainties. We believe that the true discrepancy is less extreme, probably within 3 to 6 dB. Regardless, the simulations reproduce the characteristic visual signature of the artifact in a manner sufficiently faithful to show the essential correctness of the model proposed for its formation.

DISCUSSION

The observed asymmetry (in experiment and simulation) results from the directionality of the nuclear precession. Reversing the direction of the static field (a cumbersome experiment in practice) will swap the divot from one coil to the other. This effect is most easily illustrated in the simpler case of the quadrature volume resonator (*vide supra*): reversing the sign of the imaginary drive in Eq. [1] effectively reverses the sense of precession and swaps which coil is nulled at critical coupling. The analogous result is achieved in the simulation for the surface coils by switching the signs of the imaginary components of the B_1 fields. That the location of the divot is *not* tied to the coil per se is easily demonstrated in a practical imaging experiment by physically rotating the array through an angle of π, to exchange the positions of the array members: the divot is unmoved. It is also worth noting in this context that *resistive* cross-talk can produce *no* differential shading: this follows from Eq. [1] if the input voltages at the coils are offset from each other by an arbitrary phase and the off diagonal matrix elements are made positive real.

Correction of the intensity artifact is of comparatively little interest in conventional imaging, since the visual effect is usually washed out when the images from separate coils are combined—as they invariably are for clinical viewing. However, in spectroscopic imaging, where voxel by voxel quantitation of metabolite concentrations may be required, the differential loss of intensity could cause significant errors. The method of edge completion, low pass filtering, and division, proposed by Wald *et al*. (*5*) as a means of leveling the conventional image from surface coil arrays, gives a reception profile which accounts in principal for all interactions between coils. This profile could be applied (virtually automatically) to the voxel intensities of the correspondingly combined spectroscopic data. Such a procedure introduces a T1/T2 weighting, generally undesirable, which corresponds to that of the image used to generate the correction profile; but it is likely that the net result would still be improved accuracy, relative to no correction at all. Alternative methods of generating intensity profiles based on the simulation outlined above, and using a fitting method to determine η', do not at present appear to be adaptable to the clinical setting.

EXPERIMENTAL

The coil used in this study was a homebuilt array of two elements, each in the form (roughly) of a flattened octagon (cf. Fig. 1), with linear dimensions of 7.4 by 8.4 cm (longer in the direction of overlap) and with a trace width of 0.5 cm. The overlap between elements was set empirically to minimize coupling and was 1.3 cm from center trace to center trace. The return loss, when loaded with a human head, was typically −12 to −14 dB per channel, and the conventional cross-talk was typically −14 dB, corresponding to an η of 0.2. Fiducial markers for imaging were provided by three vitamin capsules, taped to the meridian plane of array: at the center and at the left and right extremities (cf. Fig. 1).

For the cross-talk measurement of Fig. 2, we employed a pair of narrow-band preamplifiers such as are standard for proton imaging on a 1.5-T GE Signa Horizon scanner. Supply voltage to the preamps (15 V) was applied through a homebuilt bias T network, of two separate channels, with a worst-case (i.e., open circuit) isolation between channels of < -50 dB, i.e., well below the measured cross-talk. The 64-MHz carrier signal was from a PTS X10 synthesizer, and the output signals were measured on an HP 8591 spectrum analyzer, typically with a resolution bandwidth of <300 kHz, a video bandwidth of <30 kHz, and video averaging of >10 transients. The reported readings fell roughly within a range of ±0.5 dB. The measurement method was validated by terminating the array ports with 50 Ω and comparing the results to the standard cross-talk (S_{21}) measurement on an HP 8753 network analyzer; the results agreed typically to within 1 or 2 dB. Taking the network analyzer as the gold standard of measurement and factoring in the uncertainties, we estimate the cross-talk measured with the preamps loading the array to be accurate within ±2 dB.

The computer-simulated images were generated from the reciprocity principle and Eqs. [1] and [2], using field maps calculated by the Biot Savart law. Filamentary rectangular coils of dimension 8.6 × 8.0 cm were located just above a cylindrical phantom of radius 30 cm and slanted slightly down at their peripheries so as to conform to the cylinder surface. The phantom is considered to have uniform magnetization. To avoid hot spots, and to simulate the standoff from the phantom and the finite width of the actual conductors, the fields were zeroed on a radius of roughly 0.5 cm surrounding each filament. The long

dimension of the simulated coils lies in the image plane and is slightly (0.2 cm) greater than that of the actual coil; the short dimension of the simulated coil (perpendicular to the image plane) is 0.6 cm longer than that of the actual coil.

ACKNOWLEDGMENTS

This work was supported by General Electric Medical Systems and by Stifterverband der Deutschen Wissenschaft e.V., Grant TS 214/02.002/96. The authors thank Mr. Randy Hladilek , who proposed the method of cross-talk measurement with preamplifier termination. Dr. Dan Vigneron suggested the filter method of intensity correction and provided helpful comments.

REFERENCES

1. C. S. Bosch and J. J. H. Ackerman, Surface coil spectroscopy, *in* "NMR Basic Principles and Progress 27: In-Vivo Magnetic Resonance Spectroscopy II: Localization and Spectral Editing" (P. Diehl, E. Fluck, H. Günther, R. Kosfeld, and J. Seelig, Eds.), pp. 3–44, Springer-Verlag, Berlin, 1992.
2. P. B. Roemer, W. A. Edelstein, C. E. Hayes, S. P. Souza, and O. M. Mueller, *Magn. Reson. Med.* **16,** 192 (1990).
3. J. Tropp and K. Derby, *Rev. Sci. Instrum.* **62,** 2646 (1991).
4. D. I. Hoult and R. Richards, *J. Magn. Reson.* **24,** 71 (1976).
5. L. L. Wald, L. Carvajal, S. E. Moyher, S. J. Nelson. P. E. Grant, A. J. Barkovich, and D. B. Vigneron, *Magn. Reson. Med.* **34,** 433 (1995).